TELKOMNIKA, Vol. 11, No. 9, September 2013, pp. 5253~5261
ISSN: 2302-4046

Stiffness, Workspace Analysis and Optimization for 3UPU Parallel Robot Mechanism

Cui Guohua[1], Wei Bin*[2], Wang Nan[2], Zhang Yanwei[2]
[1]Department of Equipment Manufacturing, Hebei University of Engineering, Handan, 056038, China.
[2]Department of Mechanical Engineering, Hebei University of Engineering, Handan, 056038, China.
*Corresponding author, e-mail: brave.1987@163.com

Abstract

In this paper, an approach based on the particle swarm optimization is used to optimize the workspace and global stiffness of the 3UPU mechanism simultaneously due to the fact that the workspace is affected while optimizing the stiffness of the mechanism and vice versa. When optimizing one particular performance, one needs to have an objective function. Here the workspace volume of the mechanism is used as an objective function to evaluate the workspace performance of the mechanism. The leading diagonal elements of the stiffness matrix represent pure stiffness in each direction, but this stiffness changes when the moving platform position changes. We call this stiffness as local stiffness. When using the local stiffness as an objective function for stiffness optimization, it can only represent the stiffness in one particular position. Here the global stiffness of the mechanism is used as an objective function to optimize the stiffness of the mechanism. The global stiffness represents mean stiffness over the workspace.

Keywords: *parallel mechanism, workspace, global stiffness, particle swarm optimization (PSO)*

1. Introduction

Parallel mechanisms have been widely used in machine tools [1-4] and other industrial areas [5-9], this is because the parallel mechanisms possess high stiffness, high precision, good acceleration, high loading capacity, etc. The disadvantage of parallel mechanisms is the small workspace. The workspace volume can be used as an objective function for workspace optimization [10]. Stiffness is another important factor to evaluate the performance of parallel manipulators since high stiffness can lead to high precision. The leading diagonal elements of the stiffness matrix of the mechanism represent pure stiffness in each direction, but this stiffness changes when the moving platform position changes. We call this stiffness as local stiffness. When using the local stiffness as an objective for stiffness optimization, it can only represent the stiffness in one particular position; it cannot reflect the stiffness in other positions. Here the global stiffness of the mechanism is used as an objective function to optimize the stiffness of the mechanism based on the global performance index [11]. The global stiffness can represent mean stiffness over the workspace. Since the stiffness of the parallel mechanism is affected while optimizing the workspace, the global stiffness and the workspace volume of the mechanism are optimized simultaneously. There are several methods to multi-objective optimize several objective functions which are conflicting with each other [12-14], such as Pareto front theory, particle swarm optimization method, genetic algorithm, weighting objective method, etc. Here a method based on the particle swarm optimization is applied to achieve the goal.

2. Jacobian Analysis of the Mechanism

This mechanism has three translational degrees of freedom. The moving platform is connected to the base by three identical U-P-U legs. The schematic representation of the mechanism is shown in Figure 1. The fixed coordinate system $O(\mathrm{X},\mathrm{Y},\mathrm{Z})$ is attached to the center of the base, and the moving coordinate system $P(\mathrm{x},\mathrm{y},\mathrm{z})$ is attached to the center of the

Received March 25, 2013; Revised June 9, 2013; Accepted June 20, 2013

moving platform. α_b is the angle between X axis and line OB_1, α_p is the angle between x axis and line OP_1.

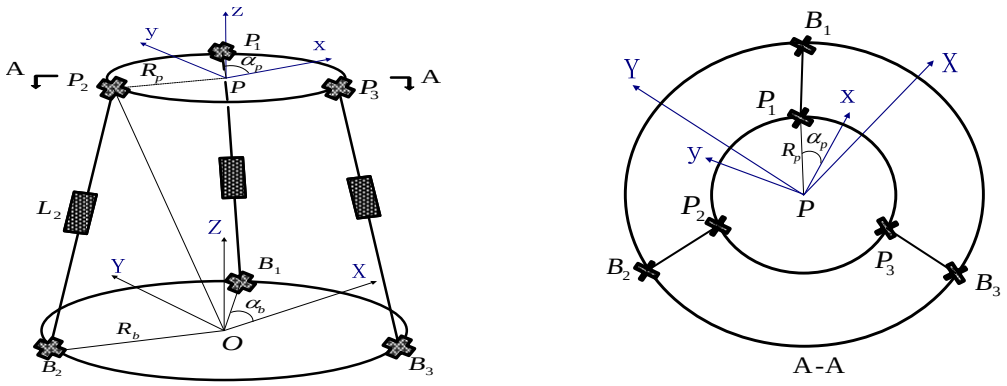

Figure 1. Schematic Representation of the 3UPU Mechanism

The coordinates of points B_i with respect to the fixed coordinate system are denoted as $b_i(i=1,2,3)$; the coordinates of points P_i with respect to the moving coordinate system are denoted as p_i. The length of each leg can be written as:

$$L_i = \left| p_i + q - b_i \right| \tag{1}$$

Where $q=[\mathrm{x},\mathrm{y},\mathrm{z}]^T$ is the vector of point P with respect to the fixed base. The velocity of point P_i can be expressed as the following:

$$v_{Pi} = \omega_i \times s_i + \dot{L}_i s_i \tag{2}$$

Where ω_i is the angular velocity of the ith leg with respect to the base and s_i is the unit vector along the ith leg. The following equation can be derived by multiplying s_i in both sides of Equation (2):

$$s_i^T v_{Pi} = \dot{L}_i \tag{3}$$

Equation (3) can be rewritten as the following:

$$Jv_P = \dot{q} \tag{4}$$

Where v_P is the velocity of the center of the moving platform. The Jabobian matrix of the mechanism can be expressed as follows:

$$J = \begin{bmatrix} s_1^T & s_2^T & s_3^T \end{bmatrix}^T \tag{5}$$

3. Workspace of the Mechanism

The workspace volume V will be used can be used as an objective function for the workspace optimization. The volume of the workspace can be computed by using fast search method [10]. When $R_b=3$, $R_p=1$, $\alpha_b=30^\circ$, $\alpha_p=15^\circ$, the workspace is shown in Figure 2(a); when $R_b=3$, $R_p=2$, $\alpha_b=30^\circ$, $\alpha_p=15^\circ$, the workspace is shown in Figure 2(b); when $R_b=2$, $R_p=2$, $\alpha_b=30^\circ$, $\alpha_p=15^\circ$, the workspace is shown in Figure 2(c); when $R_b=3$, $R_p=2$, $\alpha_b=30^\circ$, $\alpha_p=0^\circ$, the workspace is shown in Figure 2(d). The workspace volume for different structural parameters of the mechanism is listed in Table 1.

Table 1. Workspace Volume for Different Parameters of the Mechanism

	R_b	R_p	α_b	α_p	Workspace volume
Scenario (a)	3	1	30°	15°	81.8002
Scenario (b)	3	2	30°	15°	116.2673
Scenario (c)	2	2	30°	15°	146.7330
Scenario (d)	3	2	30°	0°	122.8553
Scenario (e)	3	2	20°	0°	138.5377

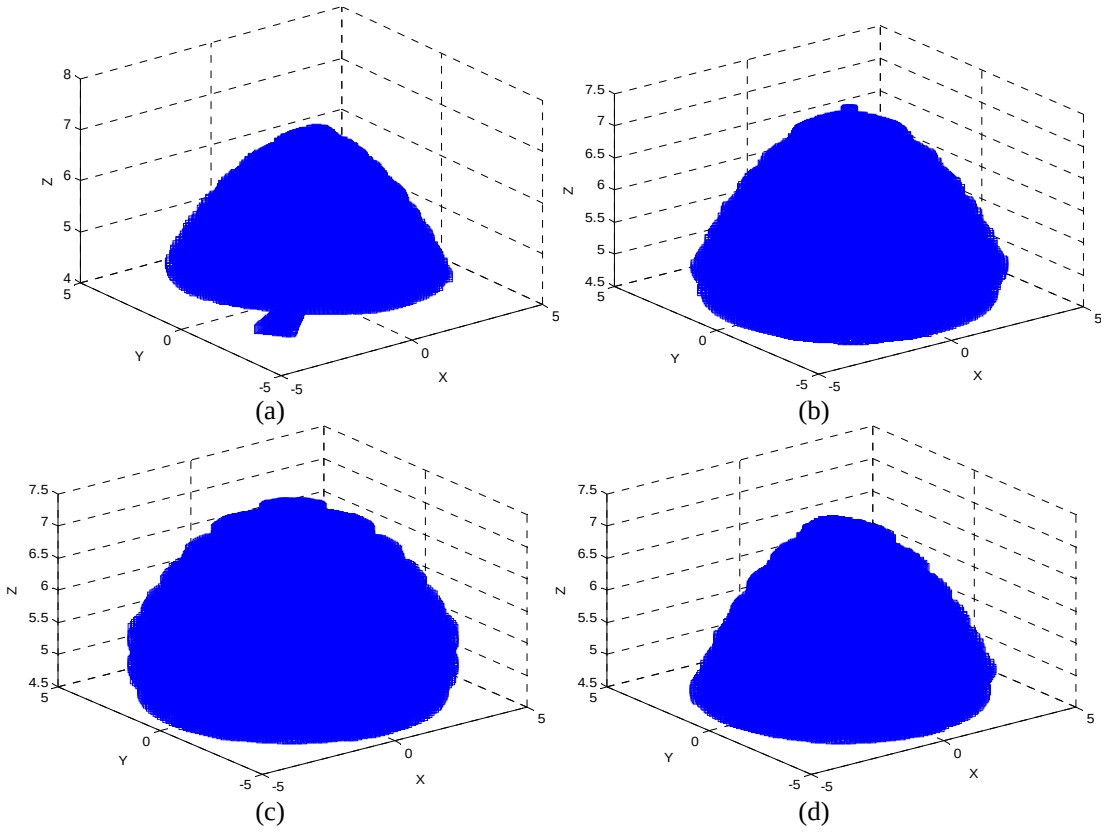

Figure 2. The workspace of the mechanism under different structural parameters

From the above figures, one can see that the radii of the base and moving platform and the location of joints on the base and moving platform all affect the size and shape of the workspace.

4. Stiffness of the Mechanism

The stiffness of a parallel mechanism at a given point in the workspace can be characterized by its stiffness matrix. The stiffness matrix can be written as follows:

$$K = J^T K_J J = k J^T J \tag{6}$$

The leading diagonal elements of the stiffness matrix are the pure stiffness in each direction. This stiffness changes when the position of the moving platform changes. We call this stiffness as local stiffness. When $\alpha_b = 30^\circ$, $\alpha_p = 15^\circ$, $R_b = 3cm$, $R_p = 1cm$, z=5cm, x=0, y=0, the stiffness matrix is the following:

$$K = \begin{bmatrix} 215.9 & 0 & 0 \\ 0 & 215.9 & 0 \\ 0 & 0 & 2568.1 \end{bmatrix}$$

From the above, one can see that the stiffness in X and Y directions is 215.9 and the stiffness in Z direction is 2568.1. This stiffness changes when the position of the moving platform changes. The stiffness mappings are illustrated in Figure 3 when $R_b = 3cm$, $R_p = 1cm$, $\alpha_b = 30^\circ$, $\alpha_p = 15^\circ$, z=5cm.

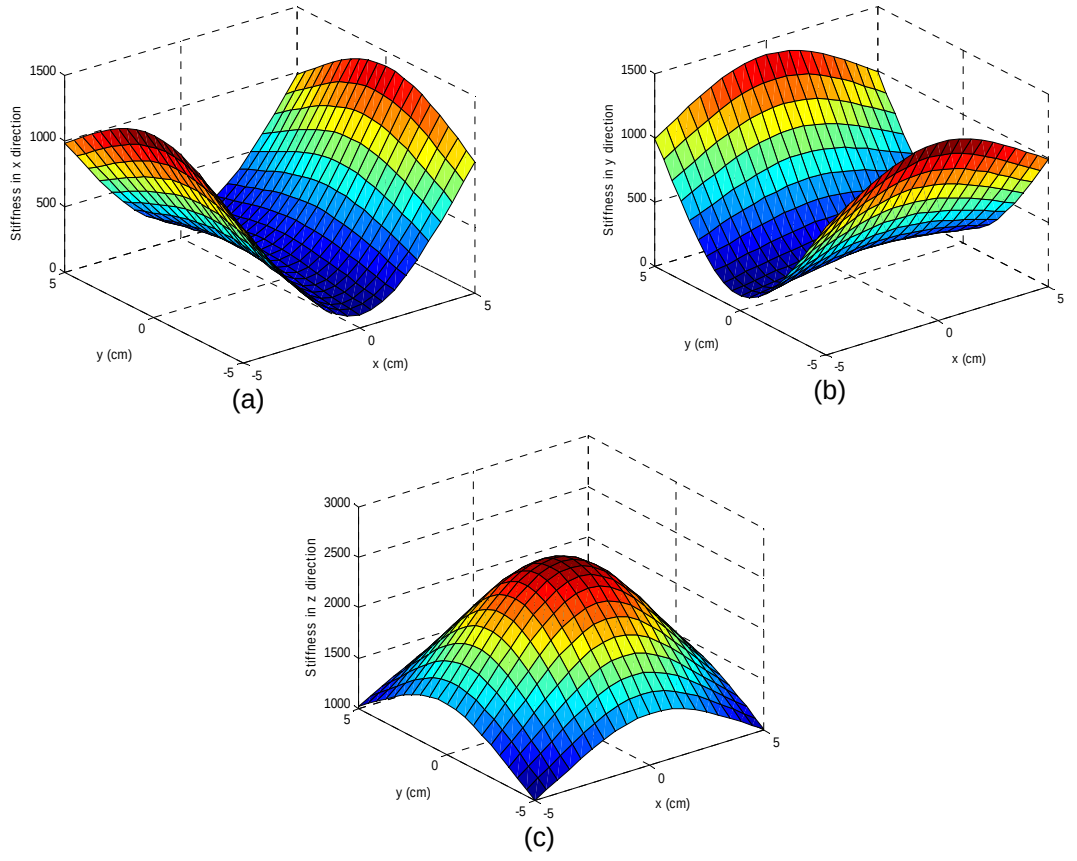

Figure 3. Stiffness in (a) X direction; (b) Y direction; (c) Z direction

From Figure 3, one can also see that the stiffness in Z direction is the maximum among those three, and the stiffness in Z direction reaches the maximum value 2568.1N/cm when x=0, y=0. If one uses the local stiffness as an objection function for optimization, it can only optimize the stiffness in one particular position; it cannot reflect the stiffness in other positions. Here the global stiffness is used as an objective function for the stiffness optimization based on the global performance index [11]. The global stiffness can represent mean stiffness in the workspace. The global stiffness can be expressed as follows:

$$GSI_x = \frac{\int\int\int K_x dxdydz}{\int\int\int dxdydz},\ GSI_y = \frac{\int\int\int K_y dxdydz}{\int\int\int dxdydz},\ GSI_z = \frac{\int\int\int K_z dxdydz}{\int\int\int dxdydz}$$

GSI_x, GSI_y and GSI_z are the global stiffness in X, Y and Z directions, respectively. When $\alpha_b = 30^\circ$; $\alpha_p = 15^\circ$, the global stiffness mappings in X, Y and Z directions with the alteration of the radii of the base R_b and moving platform R_p are shown in Figure 4. The global stiffness mappings in X and Y directions are the same.

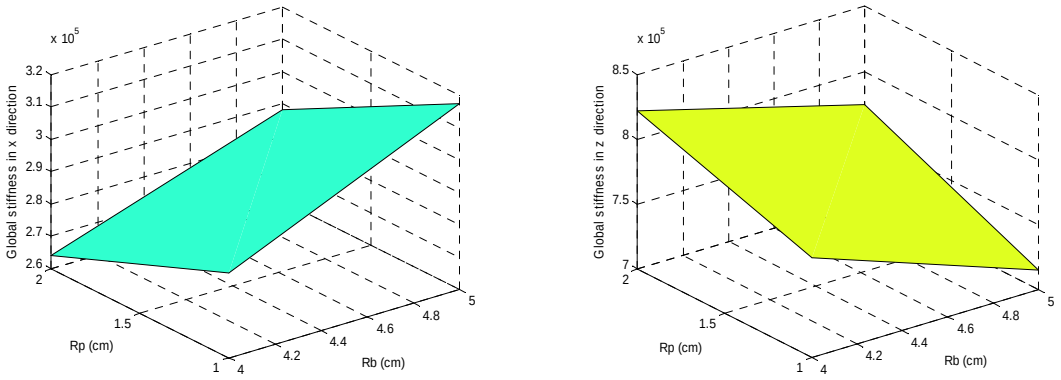

Figure 4. Global Stiffness in (a) X Direction; (b) Z Direction

When $R_b = 3cm$, $R_p = 2cm$, the global stiffness mappings in X, Y and Z directions with the alteration of the joints' location on the base α_b and moving platform α_p are shown in Figure 5. The global stiffness mappings in X and Y directions are the same.

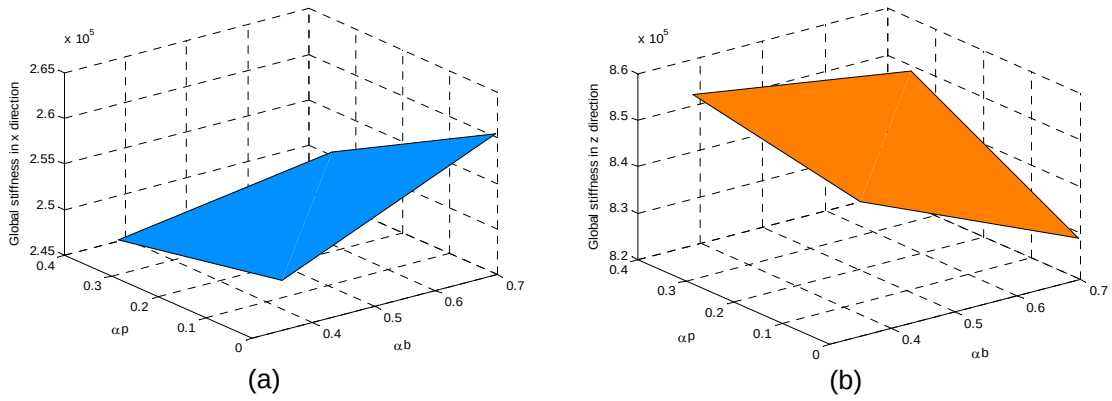

Figure 5. Global Stiffness in (a) X Direction; (b) Z Direction

From Figure 4 and Figure 5, one can see that the radii of the base and moving platform as well as the joints' location on the base and moving platform all affect the global stiffness. The mappings of the sum of global stiffness in X, Y and Z directions with the alteration of the radii of the base and moving platform and the joints' location on the base and moving platform are shown in Figure 6.

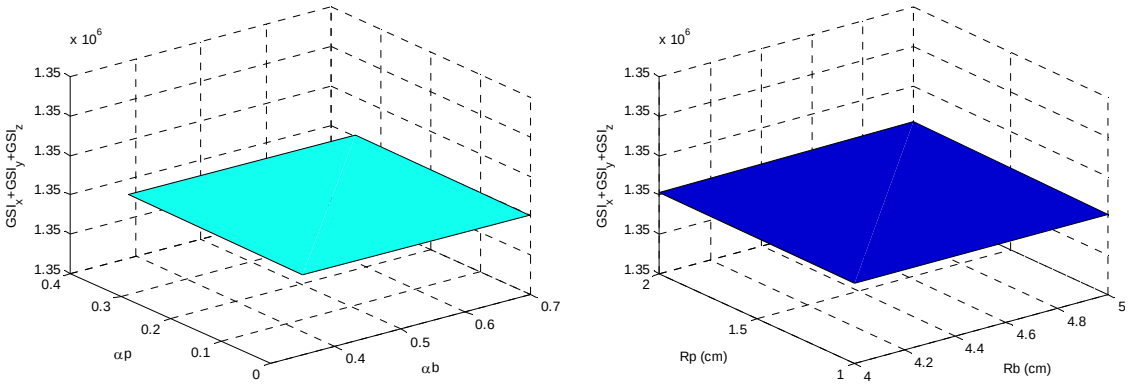

Figure 6. The Mappings of the Sum of the Global Stiffness in X, Y and Z Directions

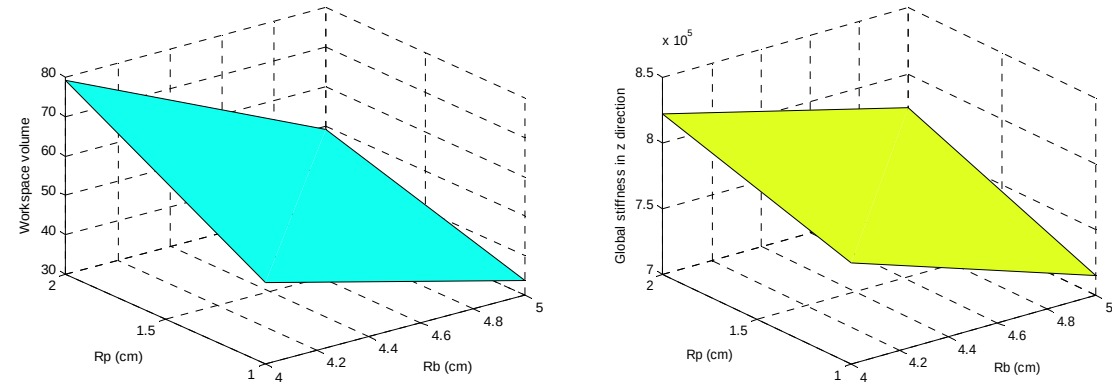

Figure 7. (a) The Workspace Volume Trend (b) The Mapping of Global Stiffness in Z direction

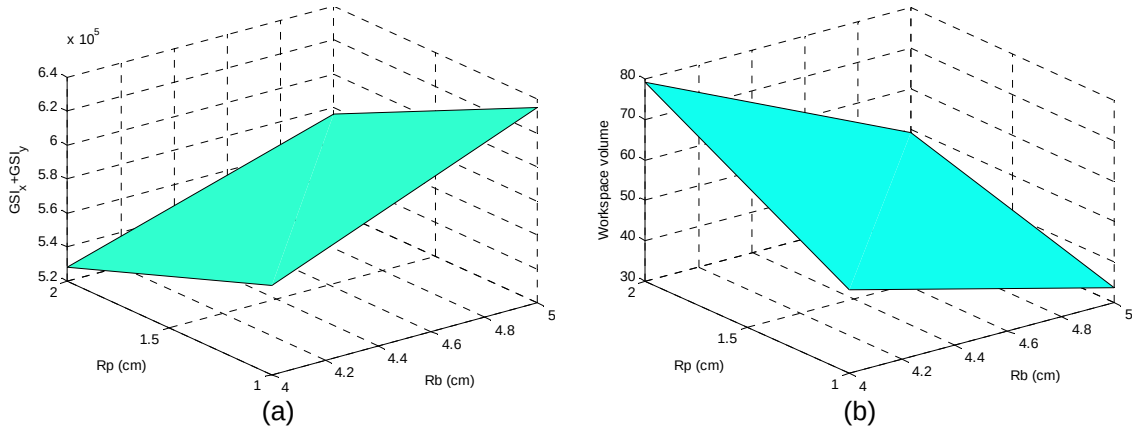

Figure 8. (a) The Mapping of the Sum of Global Stiffness in X and Y Directions
(b) The Workspace Volume Trend.

One can see that $GSI_x + GSI_y + GSI_z$ is a constant value. If we use $GSI_x + GSI_y + GSI_z$ as an objective function for stiffness optimization, that is obvious inappropriate. Some scholar proposed the stiffness in Z direction as the main stiffness and its stiffness can directly reflect the stiffness of whole mechanism [15]. So we will try to use GSI_z as an objective function for stiffness optimization.

From Figure 7 and 8, we found that the workspace volume and GSI_z have the same trend, which means these two objectives do not conflict with each other, and the workspace volume conflicts with GSI_x and GSI_y. One can just optimize the GSI_z by using like genetic algorithm. However, $GSI_x + GSI_y + GSI_z$ is a constant value, and the trends between $GSI_x + GSI_y$ and GSI_z are opposite, which means $GSI_x + GSI_y$ and GSI_z conflict with each other. If one only optimizes GSI_z, $GSI_x + GSI_y$ will be affected. So in the practical industries, engineers need to consider their own requirements to pick the right objective function for optimization. If the stiffness in Z direction is relatively important, then one can just optimize GSI_z by using like genetic algorithm. If the stiffness in X and Y direction is relatively important, one can use $GSI_x + GSI_y$ as an objective function for optimization. Here suppose the stiffness in X and Y direction is relatively important, we will optimize $GSI_x + GSI_y$ and the workspace volume simultaneously.

5. Multi-objective Optimization based on PSO

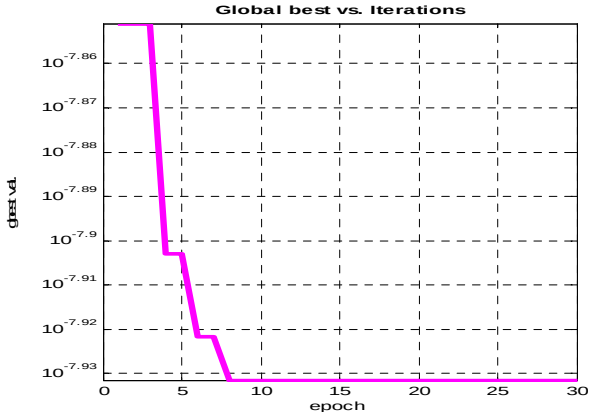

Figure 9. The $Gbest$ Value

Traditional optimization methods have the danger of falling into local optimum. If the objective function does not have the convexity property, the local optimum is therefore not the global optimum. So we will rely on the global optimization algorithm to address this issue. Particle swarm optimization (PSO) as an advanced computational intelligence method, it is inspired by simulating the swarm behavior like bird flocking. Particle swarm optimization can be viewed as the improvement of genetic algorithm. The workspace volume is used as a criterion for workspace optimization and the sum of global stiffness in X, Y directions is used as a criterion for stiffness optimization. The overall objective for optimization can be given as follows:

$$Gbest = \min \frac{1}{0.5f + 0.5V} \tag{7}$$

Where V is the workspace volume of the mechanism, and $f = GSI_x + GSI_y$ is the sum of global stiffness in X and Y directions.

Design variable are given as: R_b, R_p, α_b, α_p. Their constraints are given as follows:

$R_b \in [2,5]cm$; $R_p \in [1,3]cm$; $\alpha_b \in [20^\circ, 40^\circ]$; $\alpha_p \in [0^\circ, 20^\circ]$

The maximal velocity divisor is 2, the particles number is 24. Figure 9 shows the evolutionary process.

After optimization, R_b =3cm, R_p =3cm, $\alpha_b = 20^\circ$, $\alpha_p = 20^\circ$, $Gbest = 1.17 \times 10^{-8}$. Before optimization, R_b =4, R_p =2, $\alpha_b = 30^\circ$, $\alpha_p = 20^\circ$, $Gbest = 2.3 \times 10^{-8}$. $Gbest$ is improved 1.99 time.

6. Conclusion

An approach based on the particle swarm optimization is used to the multi-objective optimize the workspace and global stiffness of the 3UPU mechanism. The Jacobian of the mechanism is first determined, and then the workspace and global stiffness is analyzed and found that the radii of the base and moving platform as well as the joints' location on the base and moving platform all affect the workspace and global stiffness. The workspace volume of the mechanism is used as an objective function to evaluate the workspace performance of the mechanism. The sum of the global stiffness in X and Y direction is used as an objective function for stiffness optimization. The optimized results are shown that $Gbest$ is improved 1.99 times after optimization.

Acknowledgement

This work is supported by the National Natural Science Foundation of China under Grant 51075118 and 51175143.

References

[1] Lungwen T, Sameer J. Kinematic Analysis of 3-DOF Position Mechanisms for Use in Hybrid Kinematic Machines. *Journal of Mechanical Design*. 2002; 124(2): 245-253.
[2] Fengfeng X, Dan Z, Chris M. Global Kinetostatic Modeling of Tripod-based Parallel Kinematic Machine. *Mechanism and Machine Theory*. 2004; 39(4): 357-377.
[3] Dan Z, Zhuming B, Beizhi L. Design and Kinetostatic Analysis of a New Parallel Manipulator. *Robotics and Computer-Integrated Manufacturing.* 2009; 25(4-5): 782–791.
[4] Jun W, Tiemin L, Xinjun L, Liping W. Optimal Kinematic Design of a 2-DOF Planar Parallel Manipulator. *Tsinghua Science and Technology*. 2007; 12(3): 269-275.
[5] Yangming L, Qingsong X. *Kinematic Design and Dynamic Analysis of a Medical Parallel Manipulator for Chest Compression Task.* IEEE International Conference on Robotics and Biomimetics. Shatin. 2005: 693-698.
[6] Chao W, Xinjun L, Liping W. Dimension Optimization of an Orientation Fine-tuning Manipulator for Segment Assembly Robots in Shield Tunneling Machines. *Automation in Construction*. 2011; 20(4): 353-359.
[7] Min P. Improved Design of a Three-degree of Freedom Hip Exoskeleton Based on Biomimetic Parallel Structure. Master Thesis. Oshawa: University of Ontario Institute of Technology; 2011.
[8] Vincent N, Maria R, Olivier C. *Very High Speed Parallel Robot for Pick-and-Place*. IEEE/RSJ International Conference on Intelligent Robots and Systems. Edmonton. 2005: 553-558.
[9] Chao W, Xinjun L, Liping W, Jingsong W. Optimal Design of Spherical 5R Parallel Manipulators Considering the Motion/Force Transmissibility. *Journal of Mechanical Design*. 2010; 132(3): 1-10.
[10] Jian W. Workspace Evaluation and Kinematic Calibration of Stewart Platform. PhD thesis. Boca Raton: Florida Atlantic University; 1992.
[11] Clement G, Jorge A. A Global Performance Index for the Kinematic Optimization of Robotic Manipulators. *Journal of Mechanical Design*. 1991; 113(3): 220-226.
[12] Dan Z, Zhen G. Forward Kinematics, Performance Analysis, and Multi-objective Optimization of a Bio-inspired Parallel Manipulator. *Robotics and Computer-Integrated Manufacturing*. 2012; 28(4): 484-492.

[13] Abdullah K, David C, Alice S. Multi-objective Optimization Using Genetic Algorithms: A Tutorial. *Reliability Engineering and System Safety*. 2006; 91: 992-1007.
[14] Lara M, Joao R, Didier D. Multi-objective Design of Parallel Manipulator Using Global Indices. *The Open Mechanical Engineering Journal*. 2010; 4: 37-47.
[15] Bing L, Zhixing W, Ying H. The Stiffness Calculation Model of the New Typed Parallel Machine Tool. *Machine design*. 1999; 3: 14-16.
[16] Youxin L, Bin Z, Xiaoyi C. Forward Displacement Analysis of Generalized Parallel Manipulator Based on Parameter Coupled Mapping Hyper-chaotic Method. *JCIT: Journal of Convergence Information Technology*. 2012; 7(22): 468-475.
[17] Tao T, Qing G, Mingchuan Y. Support Vector Machine Based Particle Swarm Optimization Localization Algorithm in WSN. *JCIT: Journal of Convergence Information Technology*. 2012; 7(1): 497-503.